

Hydrogen Evolution Reaction at Indium Electrode in Molten Ethylammonium Tetrafluoroborate

by B. Więcek

Faculty of Chemistry, University of Wrocław, 50383 Wrocław, Poland

(Received October 31st, 2000; revised manuscript February 8th, 2001)

The hydrogen evolution reaction (HER) has been studied at indium electrode in pure molten ethylammonium tetrafluoroborate (EtNH₃BF₄). Measurements were carried out from 424 to 474 K. The a.c. impedance and potentiostatic polarization techniques were used. The exchange current density of the HER, its overall apparent activation energy, the cathodic transfer coefficient and the double layer capacitance have been determined. It has been postulated that the amine molecules do not adsorb on the indium electrode surface in the potential range applied and do not inhibit the HER.

Key words: hydrogen evolution, indium electrode, impedance spectroscopy, molten salt

It has been observed [1–4] that the electrocatalytic activity of metals for the HER is affected by a number of their solid state properties, *e.g.* work functions, the metal–metal bond energies, electronic structure of metals, *etc.* These properties determine the electrocatalytic tendencies of metals by virtue of their effect of the strength of the binding of adsorbed hydrogen atoms on a metal side. The electrocatalytic reactions, as the HER, are especially sensitive to the adsorption of other molecules at the metal electrodes. Organic molecules containing active electron–donor groups (*e.g.* –NH₂) are chemisorbed on metals with incomplete electron orbitals (*e.g.* *d*-orbitals). The adsorption of polar organic compounds can affect the rate of hydrogen evolution by blocking the electrode sites for the reaction occurring at uncovered electrode sites [5]. Our studies of the HER at platinum electrode from molten ethylammonium tetrafluoroborate (EtNH₃BF₄) showed an inhibition effect of amine molecules on the hydrogen evolution [6].

In molten alkylammonium salts alkylammonium cations are the source of hydrogen. The first step of the HER in these salts is the discharge of alkylammonium cations:



or the discharge of solvated protons H_(s)⁺:



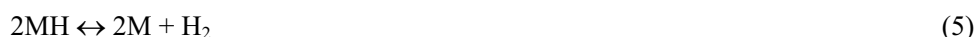
MH and B represent the hydrogen adsorbed on the electrode surface and the amine molecule, respectively. The discharge of solvated proton (2) is preceded by the dissociation of alkylammonium cation [7]:



The adsorbed hydrogen is removed from the electrode by the electrochemical desorption:



or chemical desorption:



As far as the solvated protons are discharged, the platinum electrode is not poisoned. This was observed only in molten Et_3NHBF_4 [8] and EtNH_3BF_4 in low temperature range [6,7] when alkylammonium cations are immobile. It is well known that the adsorption of organic substances depends on the nature of the metal [9]. According to an empirical equation of Pauling [10], the bond strength for a partially covalent bond of the metal with an organic species is:

$$D_{(org-M)} = \frac{1}{2} [D_{(M-M)} + D_{(org-org)}] + 23.06(\chi_{org} - \chi_M)^2 \quad (6)$$

where D is the bond strength between the respective species in $\text{kcal}\cdot\text{mol}^{-1}$ and χ is the electronegativity of the bond in Pauling units. $D_{(M-M)}$ values can be deduced from the surface energy of metal [11]. To obtain χ_M it is useful to employ the relation found by Pritchard and Skinner [12] and Gordy and Thomas [13]:

$$\chi_M = (0.40 \pm 0.07) \cdot \Phi - 0.30 \pm 0.05 \quad (7)$$

where Φ is the work function of the metal in eV. The pertaining data for platinum and indium and calculated electronegativities of both metals are listed in Table 1.

Table 1.

Metal	$D_{(M-M)}$ [11]/ $\text{kcal}\cdot\text{mol}^{-1}$	Φ [14]/eV	χ_M /eV
Pt	22.4	5.03	1.71 ± 0.40
In	9.5	4.08	1.33 ± 0.33

As can be seen in Table 1, the electronegativities of chosen metals are similar. Thus, for a given organic species the bond strength with these metals depends mainly on $D_{(M-M)}$. Hence the bond strength between platinum and given organic species might be thought to be substantially higher than for indium.

The purpose of this paper is the comparison of the influence of the adsorptive nature of the metal on the HER in molten ethylammonium tetrafluoroborate. Indium was chosen as electrode material, because the adsorbability of amine molecules on indium is expected to be lower than that on platinum [15].

EXPERIMENTAL

The ethylammonium tetrafluoroborate was obtained and purified according to the procedure described in [6,7]. The molten salt was saturated with hydrogen deoxygenated on BTS catalyzer before and throughout all measurements. A conventional two-compartment electrochemical cell was made of Pyrex glass. A fritted glass separated the compartments. An oil bath thermostat maintained the temperature of the cell constant within $\pm 0.5^\circ$. The working electrode was a drop of 99.99% pure indium, placed on a PTFE spoon. The geometrical area of the electrode was 0.65 cm^2 . The counter electrode was a platinized platinum sheet of about 10 cm^2 . The reference electrode was the reversible hydrogen electrode immersed directly in the pure fused salt. The impedance spectra were recorded under the potentiostatic mode by using a computer controlled Solartron Phase Gain Analyzer 1260 with Electrochemical Interface SI 1287. Twenty five frequencies per decade from 1 Hz up to 100 kHz at an a.c. voltage of 10 mV (peak-to-peak) were applied. The polarization measurements were performed potentiostatically using the same Solartron system.

RESULTS AND DISCUSSION

Polarization measurements. The polarization curves were obtained in a potentiostatic mode from zero to -800 mV . The typical current vs. overpotential relation is presented in Fig. 1 together with the impedance result. It is characterized by a typical for indium S-shape [1]. The extrapolation of the current density to zero overpotential was used to determine the exchange current density j_0 and the apparent cathodic transfer coefficient α_c , according to Tafel equation

$$\eta = a + b \log |j| \quad (8)$$

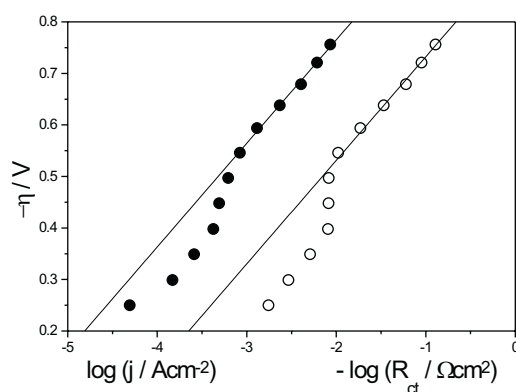
$$\text{where } a = \frac{RT}{\alpha_c nF} \ln j_0 \quad \text{and} \quad b = 2.303 \frac{RT}{\alpha_c nF} \quad (9)$$

The results are presented in Table 2.

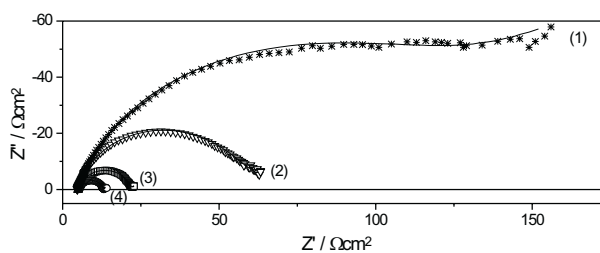
The linear part of plots has a slope around $2RT/F$ at each temperature. It implies that the HER is controlled by the electrochemical desorption step (4a) or (4b) with approximately constant coverage of hydrogen.

Table 2. The electrochemical parameters for the HER at indium electrode in molten EtNH₃BF₄ obtained from the impedance (*) and polarization (***) data.

T/K	$\log(j_0/\text{A}\cdot\text{cm}^{-2})^*$	$\log(j_0/\text{A}\cdot\text{cm}^{-2})^{**}$	α_c
424	-6.12 ± 0.04	-6.05 ± 0.06	0.42 ± 0.02
434	-5.75 ± 0.01	-5.55 ± 0.03	0.44 ± 0.01
444	-5.69 ± 0.01	-5.76 ± 0.01	0.45 ± 0.01
454	-5.17 ± 0.05	-5.45 ± 0.05	0.47 ± 0.01
464	-4.85 ± 0.02	-5.17 ± 0.02	0.42 ± 0.01
474	-4.67 ± 0.05		

**Figure 1.** Experimental: (●)Tafel and (○) η vs. $-\log R_{ct}$ plots for the HER at indium electrode in pure molten EtNH₃BF₄ at 434 K.

Impedance measurements. The impedance spectra were carried out at several potentials against the reversible hydrogen electrode from -0.2 to -0.8 V in 50 mV intervals. The measured potential values were corrected for the iR drop to obtain overpotential values. The typical recordings obtained are shown in Fig. 2.

**Figure 2.** Experimental (points) and simulated (lines) impedance spectra obtained at indium electrode in pure molten EtNH₃BF₄ at 434 K for overpotentials: (1) -0.497 V, (2) -0.594 V, (3) -0.679 V, (4) -0.756 V.

The impedance spectra were found to have the form of depressed arcs on the complex plane plots at all temperatures in the whole overpotential range studied. The obtained spectra were resolved using the impedance analysis program EQUIVCR [16] for fitting parameters of an equivalent circuit. The equivalent circuit that was found to reproduce most closely the impedance diagrams is shown in Fig. 3.

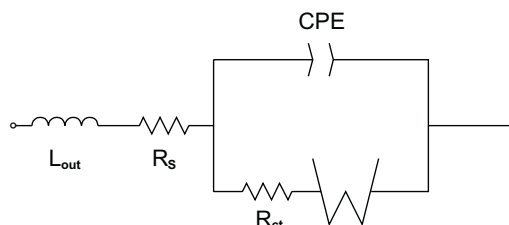


Figure 3. The equivalent circuit used in this work.

In this circuit L_{out} is the inductance due to the instrumentation and to the electrical connections between the cell and the instruments. It equals to $0.3 \mu\text{H}$. R_s is the solution resistance. They are in series with the parallel connection of the constant phase element CPE and the charge transfer resistance R_{ct} with the series connection of the Warburg impedance Z_W . The CPE substitutes the double layer capacitance and its impedance is given as [17]:

$$Z_{CPE} = \frac{1}{Q(i\omega)^{\alpha_f}} \quad (10)$$

where ω is the angular frequency of the a.c. voltage, the imaginary unit $i = \sqrt{-1}$, α_f is a constant parameter between zero and unity corresponding to a depression angle $(1 - \alpha_f) \cdot 90^\circ$ and Q is the parameter related to the average double layer capacitance C_{dl} [17] by:

$$Q = C_{dl}^{\alpha_f} (R_s^{-1} + R_{ct}^{-1})^{1-\alpha_f} \quad (11)$$

The constant phase characteristic has often been observed in experiments on solid electrodes. The capacitance dispersion is explained by fractality of the solid metal interface [18]. An electrode surface can be irregular at least in two different ways. The surface is either geometrically rough, or it is smooth, but its properties are non-uniformly distributed. The capacitance dispersion observed on the liquid indium electrode (m.p. is 429.7 K) in spite of its smooth surface is probably of interfacial origin [19,20]. The Warburg impedance representing the diffusion of the electroactive species is given by:

$$Z_W = \sigma(1 - i)\omega^{-1/2} \quad (12)$$

where σ is the Warburg coefficient. The typical results of the fitting with the mean error between the measured and model values expressed by the chi-square distribution χ^2 are presented in Table 3.

Table 3. The best-fit values of the equivalent circuit elements for the spectra presented in Fig. 2. $L_{out} = 0.3 \mu\text{H}$.

curve	η/V	$R_s/\Omega \cdot \text{cm}^2$	$Q \cdot 10^6/\Omega^{-1} \text{cm}^{-2} \text{s}^{\alpha_f}$	α_f	$R_{ct}/\Omega \cdot \text{cm}^2$	$\sigma/\Omega \cdot \text{cm}^2 \text{s}^{-1/2}$	$\chi^2 \cdot 10^4$
1	-0.497	4.6	202 ± 3	0.81	121.6 ± 1.1	111.0 ± 2.5	2.47
2	-0.594	4.7	158 ± 2	0.84	53.9 ± 0.2	12.5 ± 0.7	1.90
3	-0.679	5.1	91 ± 1	0.86	16.7 ± 0.03	2.6 ± 0.1	0.61
4	-0.756	5.1	49 ± 2	0.89	7.8 ± 0.04	1.9 ± 0.1	2.48

The shape of the spectra and the Warburg impedance obtained indicate, that for sufficiently low overpotential, diffusion mass transfer does not determine the rate of the HER. Then the cathodic current density, j , is given as [20]:

$$j = \frac{RT}{\alpha_c F} \cdot \frac{1}{R_{ct}} \quad (13)$$

where α_c is the cathodic transfer coefficient, T is the absolute temperature, R is the molar gas constant and F is the Faraday's constant. Taking α_c from the Tafel lines obtained for the steady-state polarization measurements and the charge transfer resistance from the NLLS fitting, the cathodic current density was calculated for each overpotential. The linear extrapolation of $\log(j)$ to zero overpotential was used to obtain the apparent exchange current density, j_0 , according to Tafel equation (8). The results are presented in Table 2 (together with the results of polarization method) and in Fig. 4 as a function of temperature in the Arrhenius type plot. The Arrhenius plot shows linear relationship in the whole temperature range, contrary to the results obtained in the same molten salt at platinum electrode [6,7].

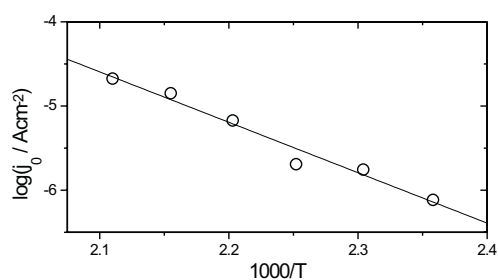


Figure 4. The Arrhenius plot obtained from impedance data for the HER at indium electrode in pure molten EtNH_3BF_4 .

It allows to calculate the overall apparent activation energy, ΔH^\ddagger , according to Arrhenius equation:

$$\Delta H^\ddagger = -\frac{\partial \ln j_0}{\partial (1/T)} \quad (14)$$

It equals to $115 \pm 10 \text{ kJ}\cdot\text{mol}^{-1}$ what is comparable with values obtained for the HER on the other *sp*-metals in molten Et_3NHBF_4 [21,22]. The typical results obtained by both methods used in the same temperature are presented in Fig. 1. This figure shows the Tafel line obtained by polarization method and the plot of η vs. $\log(1/R_{ct})$ obtained from the impedance results. Both of plots exhibit two parallel lines separated by the value of $\log(RT/\alpha_c F)$. It is obvious for the constant coverage of hydrogen atoms, where the rate of the chemical recombination step (5) becomes negligible [23]. The values obtained by both methods used are in good agreement. They are close to the results for the HER at indium electrode in molten Et_3NHBF_4 [22], where the solvated protons are discharged and the adsorption of amine molecules has not been observed. It allows supposing that the first step of hydrogen evolution at indium electrode from molten EtNH_3BF_4 is also the discharge of solvated protons.

The double layer capacitance, C_{dl} , has been estimated using equation (7). The results for four temperatures at different overpotentials are presented in Fig. 5.

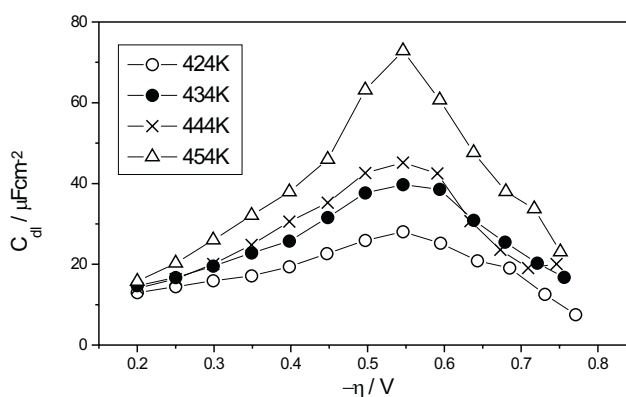


Figure 5. The double layer capacitance of indium electrode in molten EtNH_3BF_4 as a function of overpotential at different temperatures.

The double layer capacitance changes with overpotential exhibiting a maximum value at about -0.55 V . It seems, that the appearance of a characteristic peak on the capacity vs. overpotential curve [9] is connected with a desorption of ethylammonium cations from the electrode surface. The linear current – overpotential region was observed above the peak potential (see Fig. 1).

CONCLUSIONS

The first step of the HER at indium electrode from molten ethylammonium tetrafluoroborate is the discharge of solvated protons or ethylammonium cations. The exchange current density is similar to the results for indium in pure molten Et_3NHF_4 [22]. It suggests the discharge of solvated protons. The discharge of protons is preceded by dissociation of ethylammonium cations. The discharge of ethylammonium cations is not accompanied by an adsorption of amine molecules. The HER is controlled by the electrochemical desorption step. The exchange current changes with temperature according to Arrhenius equation. It indicates that the mechanism of hydrogen evolution at indium electrode in molten EtNH_3BF_4 does not change with temperature and an inhibition effect of amine molecules is not observed.

REFERENCES

1. Kita H. in "Electrochemistry; The Past Thirty and the Next Thirty Years", Bloom H., Gutmann F. Eds., Plenum Press, NY, 1977.
2. Belanger A. and Vijn A.K., *Elektrochim.*, **10**, 1854 (1974).
3. Belanger A. and Vijn A.K., *Surface Tech.*, **15**, 59 (1982).
4. Conway B.E. and Bockris J.O'M., *J. Chem. Phys.*, **26**, 532 (1957).
5. Chen L. and Lasia A., *J. Electrochem. Soc.*, **139**, 1058 (1992).
6. Więcek B., *Polish J. Chem.*, **74**, 1713 (2000).
7. Więcek B. and Kiszka A., *Polish J. Chem.*, **73**, 1323 (1999).
8. Więcek B., *Polish J. Chem.*, **67**, 2227 (1993).
9. Damaskin B.B., Petrii O.A. and Batrakov V.V. in "Adsorption of organic compounds on electrodes", Plenum Press, 1971.
10. Pauling L. "The Nature of the Chemical Bond", Cornell University Press, Ithaca, 1939, p. 60.
11. Rüetschi P. and Delahay P., *J. Chem. Phys.*, **23**, 195 (1955).
12. Pritchard H.O. and Skinner H.A., *Chem. Revs.*, **55**, 745 (1955).
13. Gordy W. and Thomas W.J.O., *J. Chem. Phys.*, **24**, 439 (1956).
14. Trasatti S., *J. Electroanal. Chem.*, **39**, 163 (1972).
15. Trasatti S., *Electrochim. Acta*, **37**, 2137 (1992).
16. Boukamp B.A., "Equivalent circuit" internal report CT89/214/128, University of Twente, 1989.
17. Brug G.J., Van den Eeden A.L.G., Sluyters-Rehbach M. and Sluyters J.H., *J. Electroanal. Chem.*, **176**, 275 (1984).
18. Nyikos L. and Paikossy T., *Electrochim. Acta*, **35**, 1567 (1990).
19. Paikossy T., *J. Electroanal. Chem.*, **364**, 111 (1994).
20. Sluyters-Rehbach M., *Pure & Appl. Chem.*, **66**(9), 1831 (1994).
21. Kiszka A. and Więcek B., *Bull. Acad. Polon. Chem.*, **34**, 153 (1986).
22. Więcek B., *Bull. Acad. Polon. Chem.*, **39**, 203 (1991).
23. Bai L., Harrington D.A. and Conway B.E., *Electrochim. Acta*, **32**, 1713 (1987).